nature communications

Article

https://doi.org/10.1038/s41467-024-50909-6

A kinase fusion protein from *Aegilops longissima* confers resistance to wheat powdery mildew

Received: 12 June 2023

Accepted: 25 July 2024

Published online: 02 August 2024

Check for updates

Huagang He[1,11] ✉, Zhaozhao Chen[1,11], Renchun Fan[2], Jie Zhang[3], Shanying Zhu[4], Jiale Wang[1], Qianyuan Zhang[1], Anli Gao[5], Shuangjun Gong[6], Lu Zhang[7], Yanan Li[2], Yitong Zhao[2], Simon G. Krattinger[8], Qian-Hua Shen[2], Hongjie Li[9,10] & Yajun Wang[7,8] ✉

Many disease resistance genes have been introgressed into wheat from its wild relatives. However, reduced recombination within the introgressed segments hinders the cloning of the introgressed genes. Here, we have cloned the powdery mildew resistance gene *Pm13*, which is introgressed into wheat from *Aegilops longissima*, using a method that combines physical mapping with radiation-induced chromosomal aberrations and transcriptome sequencing analysis of ethyl methanesulfonate (EMS)-induced loss-of-function mutants. *Pm13* encodes a kinase fusion protein, designated MLKL-K, with an N-terminal domain of mixed lineage kinase domain-like protein (MLKL_NTD domain) and a C-terminal serine/threonine kinase domain bridged by a brace. The resistance function of *Pm13* is validated through transient and stable transgenic complementation assays. Transient over-expression analyses in *Nicotiana benthamiana* leaves and wheat protoplasts reveal that the fragment Brace-Kinase$_{122\text{-}476}$ of MLKL-K is capable of inducing cell death, which is dependent on a functional kinase domain and the three α-helices in the brace region close to the N-terminus of the kinase domain.

Common wheat (*Triticum aestivum* L., $2n = 6x = 42$, AABBDD) is a widely grown cereal crop consumed by ~30% of the global population. Wheat production is constantly challenged by various fungal diseases, including rusts, *Fusarium* head blight, and powdery mildew[1]. Wheat powdery mildew, a foliar disease, is caused by the obligate biotrophic pathogen *Blumeria graminis* f. sp. *tritici* (*Bgt*) and is prevalent across most winter and spring wheat growing areas in the world, leading to significant yield losses[2–4]. *Bgt* is highly dynamic and co-evolves with wheat crops, which results in rapidly shifts in the virulence patterns of pathogen and ineffectiveness of powdery mildew resistance (*Pm*) genes used in wheat production[5,6]. Hence, exploiting and utilizing more effective *Pm* genes from common wheat and its cultivated or wild relatives are important to control powdery mildew disease[7].

[1]School of Life Sciences, Jiangsu University, Zhenjiang, China. [2]State Key Laboratory of Plant Cell and Chromosome Engineering, Institute of Genetics and Developmental Biology, The Innovative Academy of Seed Design, Chinese Academy of Sciences, Beijing, China. [3]Institute of Biotechnology and Nuclear Technology Research, Sichuan Academy of Agricultural Sciences, Chengdu, China. [4]School of Environment and Safety Engineering, Jiangsu University, Zhenjiang, China. [5]School of Life Sciences, Henan University, Kaifeng, China. [6]Institute of Plant Protection and Soil Science, Hubei Academy of Agricultural Sciences, Wuhan, China. [7]Key Laboratory of Plant Design, National Key Laboratory of Plant Molecular Genetics, Center for Excellence in Molecular Plant Sciences, Institute of Plant Physiology and Ecology, Chinese Academy of Sciences, Shanghai, China. [8]Plant Science Program, Biological and Environmental Science & Engineering Division (BESE), King Abdullah University of Science and Technology (KAUST), Thuwal, Saudi Arabia. [9]Institute of Biotechnology, Xianghu Laboratory, Hangzhou, China. [10]National Engineering Laboratory for Crop Molecular Breeding, Institute of Crop Sciences, Chinese Academy of Agricultural Sciences, Beijing, China. [11]These authors contributed equally: Huagang He, Zhaozhao Chen. ✉e-mail: hghe@ujs.edu.cn; yjwang@cemps.ac.cn

Aegilops longissima Schweinf. and Muschl. ($2n = 2x = 14$, S^lS^l) is a wild species in the Sitopsis section (S genome). It is highly related to the progenitor of the B genome of common wheat[8,9]. This diploid species is resistant to various diseases, such as rusts[10], eyespot[11], and powdery mildew[12]. The transfer of powdery mildew resistance from *Ae. longissima* into common wheat was initiated in the 1980s, leading to the creation of a series of wheat-*Ae. longissima* chromosome translocation lines[12–15].

Pm13 was mapped to the distal part of the short arm of chromosome $3S^l$, which was transferred from *Ae. longissima* into wheat chromosome 3BS[12]. This gene has not been widely used in agriculture despite its highly effective resistance to powdery mildew, which is possibly due to the linkage drag of *Pm13* introgression. Efforts have been made to reduce the *Ae. longissima* chromosomal fragments by promoting homoeologous chromosome pairing in the presence of gene *ph1b*. Cytogenetic and molecular markers were also developed to trace the critical *Ae. longissima* chromatin where *Pm13* resides[13,15,16]. However, poor chromosomal synapsis between chromosomes $3S^l$ of *Ae. longissima* and the homoeologous wheat partners limits the isolation of the target gene via the genetic recombination-based gene cloning strategies.

In this work, we report the isolation of *Ae. longissima*-originated *Pm13* using approaches that do not rely on genetic recombination, supported by transient and stable transgenic complementation assays. *Pm13* encodes a kinase fusion protein with an N-terminal domain of mixed lineage kinase domain-like protein (MLKL_NTD domain) and a C-terminal serine/threonine kinase domain bridged by a brace. Transient over-expression analysis in *Nicotiana benthamiana* leaves and wheat protoplasts reveals that the fragment Brace-Kinase$_{122\text{-}476}$ of MLKL-K is capable of inducing cell death that is dependent on kinase activity and the three α-helices in the brace region close to the N-terminus of the kinase domain.

Results

Pm13 from *Ae. longissima* confers resistance to 108 *Bgt* isolates

Non-denaturing fluorescence in situ hybridization (ND-FISH) was performed to characterize the chromosomal composition of wheat-*Ae. longissima* line No.3778, which has a pedigree of R1A/Bainong3217*5 that carries the powdery mildew resistance gene *Pm13*. Stronger signals of the FAM-labeled probe Oligo-pSc119.2 (green) were observed in the terminal regions of the short arm of chromosome 3B (3BS) compared to Chinese Spring (CS). The Tamra-labeled probe Oligo-pTa535 stained red on the rest part of chromosome 3B, which was similar to CS (Fig. 1a). This indicates that wheat line No. 3778 carries a pair of translocated chromosomes $3S^lS$-3BS.3BL, where the alien segment $3S^lS$ is introgressed onto a distal location of the wheat chromosome arm 3BS. This result is consistent with the previous cytogenetic and molecular evidence[13].

Line No. 3778 was challenged with 108 *Bgt* isolates, including 101 isolates from China and 7 isolates from European countries[3,17–19]. This line was immune (IT 0) to all *Bgt* isolates tested at the seedling stage (Fig. 1b, Supplementary Data 1). It was also highly resistant to powdery mildew in the field disease test (Supplementary Fig. 1).

Suppressed recombination between *Ae. longissima* chromosome arm $3S^lS$ and its wheat counterpart 3BS

When inoculated with *Bgt* isolate BgtYZ01, line No. 3778 showed an immune reaction (IT 0), while wheat cultivar Xumai 44 (XM44) was susceptible (IT 4). The F_1 plants from the cross between line No. 3778 and XM44 were resistant (IT 1) (Supplementary Fig. 2). The F_2 population, consisting of 238 plants, segregated into 182 resistant plants (IT 0 or 1) and 56 susceptible plants (IT 4), fitting a 3:1 segregation ratio ($\chi^2 = 0.275$, $P = 0.600$). This demonstrates that the seedling resistance of line No. 3778 to isolate BgtYZ01 is controlled by an incompletely dominant gene.

Thirty-seven polymorphic molecular markers were developed based on 57 single-copy or low-copy ($E = 10^{-5}$) genes from the 0–22 Mb region of chromosome $3S^l$ of *Ae. longissima* accession AEG-6782-2 reference genome (Supplementary Data 2). Four co-dominant markers, *X1650*, *X3140*, *X3990,* and *X5730*, spanning ~16 Mb of $3S^lS$, were linked to the resistance phenotype (Supplementary Data 3). This suggests that the introgressed chromosomal segment of *Ae. longissima* $3S^lS$ shows suppressed recombination with its wheat counterpart 3BS, indicating that the No. 3778/XM44 population is not suitable for finely mapping *Pm13*.

Physical mapping of *Pm13* using radiation-induced chromosomal aberrations

A mutant population of line No. 3778 was generated using ^{60}Co-γ-ray irradiation. Ten susceptible mutant lines, designated m1–m10, were identified from 424 M_2 families (Supplementary Data 4). The phenotypes of these mutants were confirmed by reassessment of disease resistance with their M_3 plants (Fig. 1c). These mutants were genotyped with the 37 molecular markers mentioned above. The presence and absence of these markers defined eight types of structural aberrations representing different sizes of chromosomal deletions (Fig. 1d). These markers failed to amplify any products from the mutant lines m1–m3, suggesting the absence of the *Ae. longissima* chromosomal segment $3S^lS$. Mutant lines m4 and m5 harbored chromosomal deletions with different sizes of segments from the proximal side, with breakpoints flanked by markers *X2410*/*X2520* and *X2150*/*X2250*, respectively. Mutant lines m7–m10 carried chromosomal segment deletions from the distal side, with breakpoints flanked by markers *X4150*/*X4220*, *X3940*/*X3990*, *X3410*/*X3520* and *X2770*/*X2820*, respectively. Line m6 harbored a chromosomal deletion with breakpoints defined by markers *X2020*/*X2150* and *X4150*/*X4220* (Fig. 1d). Since all mutants were susceptible to isolate BgtYZ01, *Pm13* was localized in an interval flanked by markers *X2410*/*X2820*.

Markers *X2410* and *X2820* correspond to *Ae. longissima* genes *AE.LONG.r1.3SG0172410* (Chr$3S^l$: 3,709,741–3,711,655 bp) and *AE.LONG.r1.3SG0172820* (Chr$3S^l$: 4,446,231–4,448,390 bp), respectively, in the *Ae. longissima* AEG-6782-2 reference assembly, delimiting *Pm13* to a 0.74-Mb interval containing 25 high-confidence genes and 15 low-confidence genes. Four genes were possibly associated with plant disease resistance, including three nucleotide-binding leucine-rich repeat receptor (NLR) genes (*AE.LONG.r1.3SG0172500*, *AE.LONG.r1.3SG0172570* and *AE.LONG.r1.3SG0172580*), and one receptor-like kinase gene (*AE.LONG.r1.3SG0172810*).

MLKL_NTD domain-containing kinase gene *MLKL-K* is the *Pm13* candidate

To isolate *Pm13*, we screened 326 EMS-induced M_2 families of line No. 3778 and obtained six independent susceptible mutant lines (m11–m16) (Fig. 2a, Supplementary Data 4). We sequenced the *Bgt*-infected leaf transcriptomes of the wild-type (WT) line No. 3778 and six susceptible mutants by generating an average of 72.2 million 150-bp paired-end RNA-Seq reads (21.6 Gb) per sample. Sequence reads of the six mutant lines were mapped against the assembled transcriptome of the WT parent to look for transcripts that carry single nucleotide polymorphisms in multiple mutants[20].

This approach revealed a 2006 bp transcript, designated NODE_25350_length_2006_cov_24.294361_g11779_i0 (NODE_25350 for short), which carries the EMS-type point mutations (G to A or C to T) in five out of the six sequenced mutants (Fig. 2a, Table 1). Three out of the four candidate genes within 0.74-Mb interval were retrieved from the assembled transcriptome of the WT parent; however, only the transcript NODE_4312_length_3556_cov_17.726385_g2262_i0 (NODE_4312 for short), which corresponds to the NLR gene *AE.LONG.r1.3SG0172580*, carries one EMS-type point mutation (G to A) in m13 (Fig. 2a, Table 1). No mutations were found in transcripts that corresponds to

https://doi.org/10.1038/s41467-024-50909-6

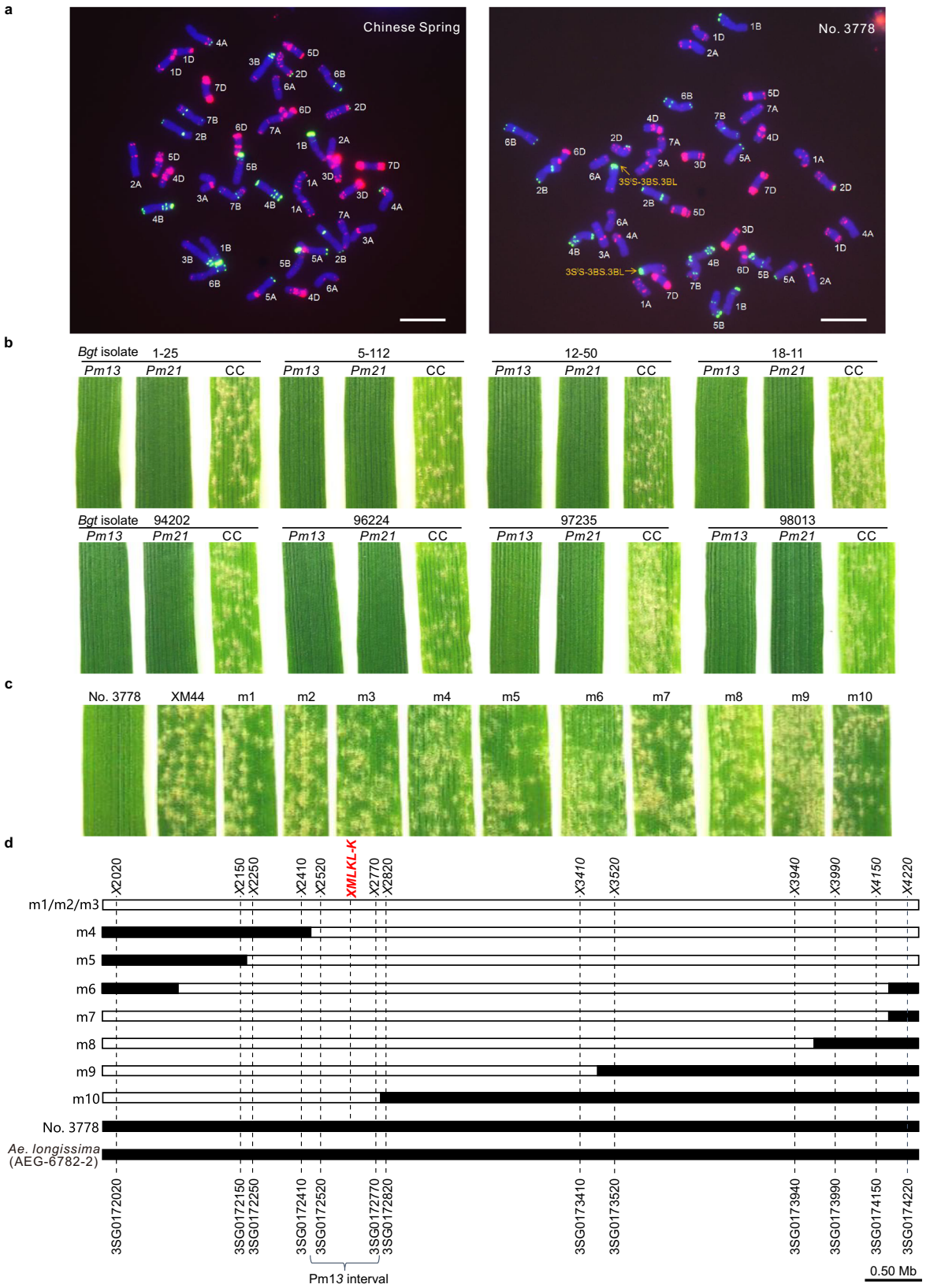

the other NLR gene and the receptor-like kinase gene. As EMS mutagenesis usually produces one mutation in 20–40 kb on average in wheat[21], the probability of the transcript NODE_25350 (2006 bp) being mutated across five *Pm13* mutants by chance is 7.96×10^{-9}, while the probability of finding one EMS-type mutation in transcript NODE_4312 (3556 bp) from six *Pm13* mutants is 0.129[20,22].

We searched for NODE_25350 in the genomes of *Ae. longissima* accessions AEG-6782-2 and TL05. A putative homologous genomic sequence was found in an unanchored sequence (chrUn: 3,336,888–3,345,975 bp) in accession AEG-6782-2, but no gene was annotated from it. We did not find any homologous sequence or gene that corresponds to NODE_25350 in accession TL05. Orthologous

Fig. 1 | Physical mapping of the highly effective *Pm13*. **a** Non-denaturing fluorescence in situ hybridization (ND-FISH) patterns of Chinese Spring (left) and line No. 3778 (right). Chromosomes of Chinese Spring and No. 3778 were stained with 4′,6-diamidino-2-phenylindole (DAPI) (blue), Oligo-pSc119.2 (green), and Oligo-pTa535 (red). Orange arrows indicate the translocated chromosomes 3S^{l}S-3BS.3BL. The experiment was independently repeated three times with consistent results. Scale bar = 10 μm. **b** Representative images showing phenotypic effects of *Pm13* against 8 out of 108 tested *Bgt* isolates. Line No. 3778 carrying *Pm13*, YM18 carrying *Pm21*, and Chancellor (CC) without any *Pm* gene were inoculated with the indicated isolates. Leaves are shown sequentially from left to right. **c** Representative images showing powdery mildew symptoms on susceptible γ-ray irradiation-induced M_3 mutants (IT4), the resistant parent line No. 3778 carrying *Pm13* (IT0), and the susceptible control XM44 (IT4). Powdery mildew responses of mutants were examined at the M_2 and M_3 generations. **d** Physical mapping of *Pm13* using chromosomal deletion mutant lines. Dot lines show the positions of markers and corresponding genes in the reference genome of *Ae. longissima* accession AEG-6782-2. The red marker was developed from the *Pm13* candidate transcript NODE_25350. Black and white bars indicate the presence or absence of markers.

genes corresponding to NODE_25350 were found in other Sitopsis species of *Aegilops*, including *Ae. bicornis.TB01.3S01G001680O0*, *Ae.searsii.TE01.3S01G001630O0*, *Ae.sharonensis.TH02.3S01G001360O0*, and *Ae.speltoides.TS01.3B01G0036300*. The collinear positions of these orthologous genes fell into the 0.74-Mb physical interval of *Pm13* (Supplementary Fig. 3, Supplementary Data 5). Marker *XMLKL-K* (Supplementary Data 6) developed from NODE_25350 was present in the WT line No. 3778, but absent in all ten irradiation-induced mutants (Fig. 1d, Supplementary Fig. 4). These results indicate that the corresponding gene of NODE_25350 is located in the *Pm13* physical interval.

Primers (Supplementary Data 6) designed on NODE_25350 and conserved sequences of the Sitopsis species of *Aegilops* were used to isolate the 11,376 bp genomic sequence of *MLKL-K* from line No. 3778, including a 2637 bp promoter, a 6554 bp encoding region consisting of seven exons and six introns (Fig. 2b) and a 1932 bp terminator. RT-PCR using cDNAs of line No. 3778 and subsequent Sanger sequencing revealed identical transcript sequence to NODE_25350. NODE_25350 contains a 1431 bp open reading frame that encodes a predicted 476 amino acid protein with an N-terminal domain of mixed lineage kinase domain-like protein (MLKL_NTD domain)-containing serine/threonine kinase, designated MLKL-K. Its kinase domain belongs to the LRR_8B subfamily (cysteine-rich receptor-like kinases), which is the most frequent kinase subfamily found in kinase fusion proteins[23]. The mutations in the five EMS-induced mutants were validated by Sanger sequencing, and they led to five amino acid (AA) substitutions in the kinase domain of MLKL-K (Fig. 2b). Three AA substitutions were aligned to the EMS-induced AA substitutions of kinase-fusion proteins reported before (m13: G231R aligns to G45R in SNN3-D1 and G90E in WTK6-vWA, m16: C334Y aligns to C166Y in Sr43 and C195Y in WTK6-vWA, m15: P461L aligns to P349L in WTK6-vWA), and the other two were adjacent to the reported ones (m12: G308E adjacent to G132D in Pm4 and S170N in WTK6-vWA, m11: G401D adjacent to A234V in Sr43 and T211I in Yr36) (Supplementary Fig. 5)[20,24–37]. Mutant m14 had no change in the coding sequence (CDS) of *MLKL-K*, which might have a mutation in the regulatory region or other genes associated with the powdery mildew resistance conferred by *Pm13*.

We isolated 15 *MLKL-K* alleles from the cDNAs of 21 *Ae. longissima* accessions showing immunity to BgtYZ01. These alleles have nucleotide identities of 97.8% to 100% compared to *MLKL-K* from line No. 3778. These encoded MLKL-Ks exhibited amino acid sequence identities of 96.0% to 100%, compared to MLKL-K from line No. 3778 (Supplementary Data 7).

MLKL-K is sufficient for powdery mildew resistance

Biolistic bombardment-based single-cell transient over-expression of *MLKL-K* CDS in the epidermal cells of susceptible wheat cv. XM44 significantly reduced the haustorium index (36.8%) of *Bgt* isolate E09 infection compared to the empty vector as the negative control (67.5%), while over-expressing of the positive control *Pm21* resulted in a haustorium index (33.7%) comparable to *MLKL-K* (Fig. 2d, Supplementary Data 8). Subsequently, the construct containing the *MLKL-K* CDS under the control of its native promoter (2637 bp) and native terminator (1932 bp) (Fig. 2c) was transformed into the susceptible wheat cv. Fielder via the *Agrobacterium*-mediated transformation. Seven independent *MLKL-K*-positive transgenic T_0 plants, verified by the diagnostic marker *XMLKL-K*, showed an immune reaction when inoculated with isolate BgtYZ01, while non-transgenic Fielder plants were susceptible (Fig. 2e, Supplementary Fig. 6). The derived seven T_1 families displayed a resistance/susceptibility segregation when challenged by BgtYZ01. Molecular analysis using marker *XMLKL-K* revealed that the presence of the transgene was associated with the resistant phenotype, and the absence of transgene was associated with the susceptible phenotype (Fig. 2f). Furthermore, all marker-positive T_1 plants from T_1-line 1 and T_1-line 2 were resistant to 20 tested *Bgt* isolates (Supplementary Fig. 7). The expression of *MLKL-K* in seven T_1 plants was also confirmed by qPCR (Supplementary Fig. 8). Collectively, these results demonstrate that the candidate gene *MLKL-K* is sufficient for the resistance to wheat powdery mildew and is the causal gene of the *Pm13* locus.

Truncated MLKL-K is capable of inducing cell death

T_1 transgenic plants expressing *MLKL-K* were grown until the heading stage in a greenhouse. Comparison of transgene-positive and negative siblings revealed that *MLKL-K* did not have any apparent deleterious effect on plant development or cause spontaneous cell death in wheat cultivar Fielder (Supplementary Fig. 9a, b). We inoculated *MLKL-K* donor line No. 3778 and susceptible control XM44 with *Bgt* isolate E09. At 48 h post-inoculation (hpi), H_2O_2 accumulation and cell death were observed in the infected epidermal cells of No. 3778 but not in XM44 (Supplementary Fig. 10). This suggests that MLKL-K can prevent the colonization of *Bgt* by inducing H_2O_2 accumulation and host cell death.

To study the resistance mechanism of MLKL-K at the biochemical level, we first used AlphaFold v2.0 to predict the three-dimensional structure of MLKL-K. This protein contains an N-terminal MLKL_NTD domain consisting of a four-helix bundle (4HB), a central three-helix-containing brace loop and a C-terminal serine/threonine kinase (STK) domain (Fig. 3a). No signal peptide was predicted for MLKL-K. Localization experiments in wheat protoplasts and epidermis cells of *N. benthamiana* indicated that MLKL-K might localize in the cytoplasm and nucleus (Supplementary Fig. 11). We then infiltrated *Agrobacteria* carrying constructs of full-length *MLKL-K* or different truncated fragments (Fig. 3b) into *N. benthamiana* leaves independently. Only the fragment Brace-kinase$_{122\text{-}476}$ resulted in strong cell death. The full-length MLKL-K (MLKL-K_FL$_{1\text{-}476}$), single MLKL_NTD domain (MLKL_NTD$_{1\text{-}136}$), brace region (Brace$_{122\text{-}217}$), kinase domain (Kinase$_{218\text{-}476}$) and MLKL_NTD-Brace$_{1\text{-}217}$ did not trigger cell death (Fig. 3c, Supplementary Fig. 12a and 13). The kinase-dead version Brace-Kinase$_{122\text{-}476}$D367A (mutated in the ATP-binding pocket) failed to trigger cell death (Fig. 3d, Supplementary Fig. 14). Similarly, the expression of Brace-Kinase$_{122\text{-}476}$ with point mutations (G231R, G308E, C334Y, G401D and P461L) from five EMS mutants also showed abolished cell death (Supplementary Fig. 15), which correlates with abolished resistance to BgtYZ01 in EMS mutants. These results suggest that Brace-Kinase$_{122\text{-}476}$-induced cell death is dependent on the functional kinase domain and is associated with powdery mildew resistance in wheat.

We also observed that the intensity of Brace-Kinase$_{122\text{-}476}$-induced cell death appeared to be associated with the number of helices in the brace region. In the transient expression experiments of both *N. benthamiana* leaves and wheat protoplasts, the kinase domain with three helices (α1-α2-α3-Kinase$_{160\text{-}476}$) induced stronger cell death than the

https://doi.org/10.1038/s41467-024-50909-6

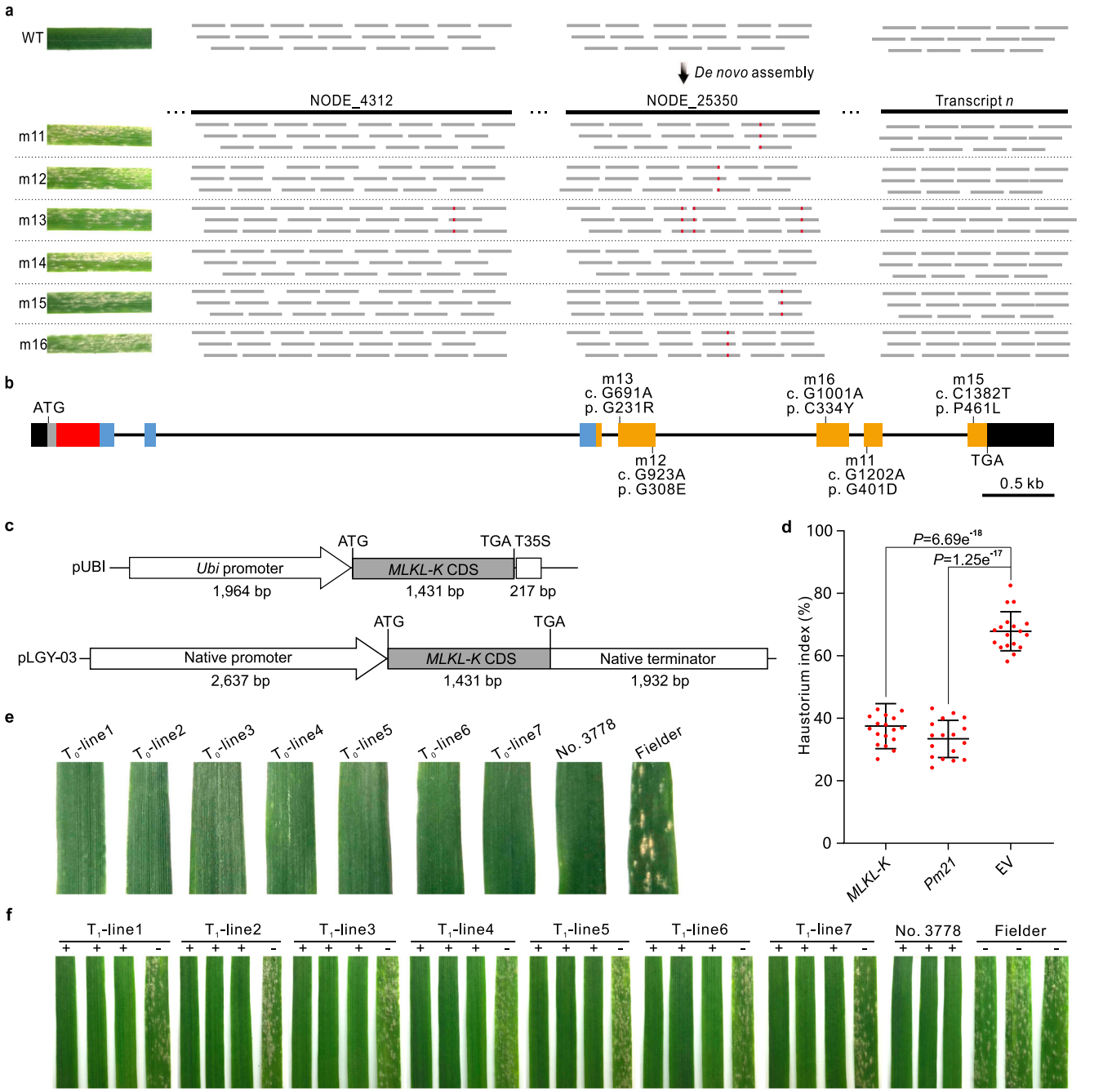

Fig. 2 | Identification, characterization and functional validation of *Pm13*. **a** Schematic representation of transcriptome sequencing analysis of EMS-induced loss-of-function mutants. The de novo assembly of the WT transcriptome was used as a reference. Powdery mildew inoculation of mutants was performed at the M_2 and M_3 generations (IT4). **b** The structure of the candidate gene of *Pm13*. Exons are represented as rectangular bars, and introns are shown as black lines between exons. Predicted protein domains are indicated by different colors: red for N-terminal domain of mixed lineage kinase domain-like protein (MLKL_NTD), blue for brace region, orange for serine/threonine kinase domain, gray for unidentified protein region, and black for 5′ UTR and 3′ UTR. Positions of EMS-type point mutations identified are indicated by short bars. **c** Schematic diagram of two constructs with the CDS of the *Pm13* candidate gene *MLKL-K* driven by the maize *Ubi* promoter and its native promoter. These constructs were used to transiently transform epidermal cells of susceptible wheat cv. XM44 and stable transform susceptible wheat cv. Fielder, respectively. **d** The haustorium index of *MLKL-K*, *Pm21*, and the empty vector (EV) in transiently transformed cells challenged by isolate E09. Each red dot represents one bombarded leaf (*MLKL-K*: n = 17, *Pm21*: n = 17, and EV: n = 18). Haustorium index values are means ± SD from 17 to 18 biological replicates. Error bars represent standard deviations based on 17 to 18 biological replicates. *P* values were calculated with a two-tailed Student's *t*-test. **e** Responses of seven independent T_0 transgenic lines expressing *Pm13* to isolate BgtYZ01 at the adult-plant stage. Line No. 3778 and the recipient Fielder were used as the resistant and susceptible controls. **f** Responses of the seven corresponding independent T_1 transgenic families to *Bgt* isolate BgtYZ01 at the seedling stage. Symbols '+' and '−' represent siblings from each family with and without transformed *MLKL-K*, respectively. The experiment was performed with four plants (three transgene-positive and one negative) selected from ten T_1 seedlings of each family. Source data are provided as a Source Data file.

Table 1 | Number of transcripts with *n* EMS-induced point mutations in the six sequenced EMS-induced mutants of line No. 3778

	Number of transcripts
Number of transcripts mutated in 0 lines	133,208
Number of transcripts mutated in 1 line	5902[a]
Number of transcripts mutated in 2 lines	229
Number of transcripts mutated in 3 lines	7
Number of transcripts mutated in 4 lines	0
Number of transcripts mutated in 5 lines	1[b]
Number of transcripts mutated in 6 lines	0

[a]Number of transcripts carries point mutations in one (NODE_4312) out of the six sequenced mutants.
[b]Transcript NODE_25350 carries point mutations in five out of the six sequenced mutants.

kinase domain with two helices (α2-α3-Kinase$_{174-476}$), and the kinase domain with only one helix (α3-Kinase$_{194-476}$) did not trigger any cell death (Fig. 3d, e, Supplementary Fig. 12b and 14). These results suggest that Brace-Kinase$_{122-476}$ mediated cell death requires a functional kinase domain and the helices in the brace region.

MLKL-K/Pm13 originates from a recent fusion event of the kinase and MLKL_NTD domains

Using the amino acid sequence of the MLKL_NTD domain of MLKL-K/Pm13, we performed a BLAST against the proteomes of the tribe Triticeae and other plant species. The matched proteins were annotated by the NCBI Conserved Domain Search. We found that various types of MLKL_NTD-containing proteins exist in the plant kingdom. MLKL_NTD-PLAC8 (MLKL_NTD fused to PLAC8 domain) is the most common type, widely distributed among plant species across the gymnosperms, eudicots and monocots. Only in Poaceae, we found other types of MLKL_NTD-containing proteins, including proteins containing a single MLKL_NTD domain or two tandem MLKL_NTD domains, MLKL_NTD fused with STK (MLKL-K-like proteins), WD40 domain, BRX domain and NLR proteins (Supplementary Data 9 and 10). This indicates the rapid evolution of MLKL_NTD-containing proteins in Poaceae.

We found that the MLKL-K-like protein family may have expanded and become the major type of MLKL_NTD domain-containing proteins in the tribe Triticeae, which contains 11 to 34 members per species (Supplementary Fig. 16, Supplementary Data 10). Phylogenetic analysis based on the kinase domains showed that MLKL-K-like proteins were clustered into three distinct clades, indicating that the fusion of the kinase and MLKL_NTD domains occurred at least three times during the evolution of the Poaceae plants. MLKL-K/Pm13 and its orthologs were only found in the Sitopsis species of *Aegilops*, encoded by single-copy genes of the S-genome, while the other two kinase-MLKL_NTD fusion events were observed across different grass species (Supplementary Fig. 16). This suggests that MLKL-K/Pm13 and its orthologs originate from a relatively recent kinase-MLKL_NTD fusion event.

Discussion

The *Ae. longissima* sourced *Pm13* exhibited a wide spectrum of resistance to wheat powdery mildew, as tested by a collection of *Bgt* isolates from China and the European countries. Suppressed recombination between the alien chromosomal arm 3S^{l}S and the wheat homoeologous chromosomal arm 3BS limits the map-based cloning of *Pm13*. Irradiation with γ-ray is often used to create small segment translocation lines in wheat[38,39]. It can also produce different sizes of chromosomal deletions surrounding genes of interest, which we have used to physically map and identify *Pm12*[19]. We developed a set of powdery mildew-susceptible chromosomal deletion lines that were used to map *Pm13* to a 0.74-Mb interval containing 40 annotated genes in the reference genome of *Ae. longissima* accession AEG-6782-2. This again proved that γ-ray-mediated chromosomal aberrations could effectively map genes located in suppressed recombination regions.

Several genomics-assisted gene cloning tools have been developed to rapidly isolate disease resistance genes. For example, MutChromSeq, based on chromosome flow sorting, was used to isolate *Pm2*[22], *Pm4*[34], *Lr14a*[40], and *Rph1*[41]. Ten NLR genes have been cloned using MutRenSeq, which combines mutagenesis, resistance gene enrichment, and sequencing[42–48]. MutChromSeq requests genetic mapping and technically demanding chromosome sorting, while MutRenSeq is suitable only for cloning NLR-type resistance gene. Recently, *Lr9*/*Lr58* and *YrNAM* were cloned using the transcriptome sequencing-based MutIsoSeq[20] and sequencing trait-associated mutations (STAM)[49], respectively. Both methods allow direct linkage of the phenotype of disease resistance with its causal transcripts and does not rely on recombination or genetic mapping. They both used full-length transcripts from PacBio Isoseq as references. For the cloning of *Pm13*, we used Illumina RNA-Seq and de novo transcriptome assembly to generate the reference, which makes the method more cost-effective.

Among the 85 disease resistance genes isolated from wheat and its relatives, 48 genes encode intracellular NLRs, 7 genes encode cytomembrane-localized receptor-like kinases (RLKs), and 16 genes produce different types of kinase fusion proteins (KFPs), including tandem kinases consisting of kinase and pseudokinase, and single or tandem protein kinases fused to other domains, such as integrated NLR, teroidogenic acute regulatory protein-related lipid transfer domain (START), and von Willebrand factor A domain (vWA)[20,29,36,50–52] These KFPs have emerged as a new type of receptor involved in the innate immunity in the Triticeae species[36]. *MLKL-K/Pm13* encodes a KFP whose putative functional STK domain is fused in the C-terminus of a unique MLKL_NTD domain, which is consistent with the recent report that was published during the consideration of this paper[53]. Protein kinase proteins are apparent targets of pathogen invasion, and they could duplicate themselves to provide decoys for effectors[54]. Such decoys work with or integrate with R proteins to convey resistance[54–56]. Phylogenetic analysis shows that the high copy number of MLKL-K-like proteins in the Triticeae plants might result from three domain fusion events and multiple gene duplications. We hypothesize that MLKL-K-like proteins played a role in plant immunity. During the arm race between hosts and pathogens, these MLKL-K-like proteins could be targeted by pathogen virulence effectors. Their MLKL-NTD domains could be the binding sites of effectors, which were fused to a functional kinase domain as an 'integrated decoy', resulting in the new resistance gene *MLKL-K*[20,36,56].

Animal MLKLs, *Arabidopsis* MLKLs (AtMLKLs) and MLKL-Ks share a similar structure of an N-terminal four-helix bundle (4HB) and a C-terminal kinase domain bridged by a brace[57]. However, both the N-terminal four-helix bundle Animal MLKLs and MLKL-K were annotated as MLKL_NTD (CDD cd21037) using NCBI Conserved Domain Search, while the counterpart of AtMLKLs was annotated as DUF1221 (CDD cl06017). Both animal and *Arabidopsis* MLKLs have pseudokinase domains that are classified as a dual specificity tyrosine-serine/threonine kinase, while plant MLKL-Ks contain a putatively functional serine/threonine kinase domain. Moreover, MLKL-Ks only occur in Poaceae species. These results indicate that plant MLKL-Ks have evolved independently.

In *Arabidopsis*, *Atmlkl* mutants exhibit an increased susceptibility to the obligate biotrophic fungus *Golovinomyces orontii*, which causes powdery mildew of *Arabidopsis*. Structural analysis suggests that AtMLKL retains an auto-repressed tetramer state[57]. During Toll-interleukin-1 receptor domain NLR (TNL)-receptor-triggered immunity, the EDS1-SAG101 complex facilitates AtMLKL clustering at the plasma membrane, leading to 4HB-dependent sustained cytoplasmic Ca^{2+} influx and subsequent immune responses[58]. MLKL is the most terminal obligatory component of the necroptosis cell death pathway

https://doi.org/10.1038/s41467-024-50909-6

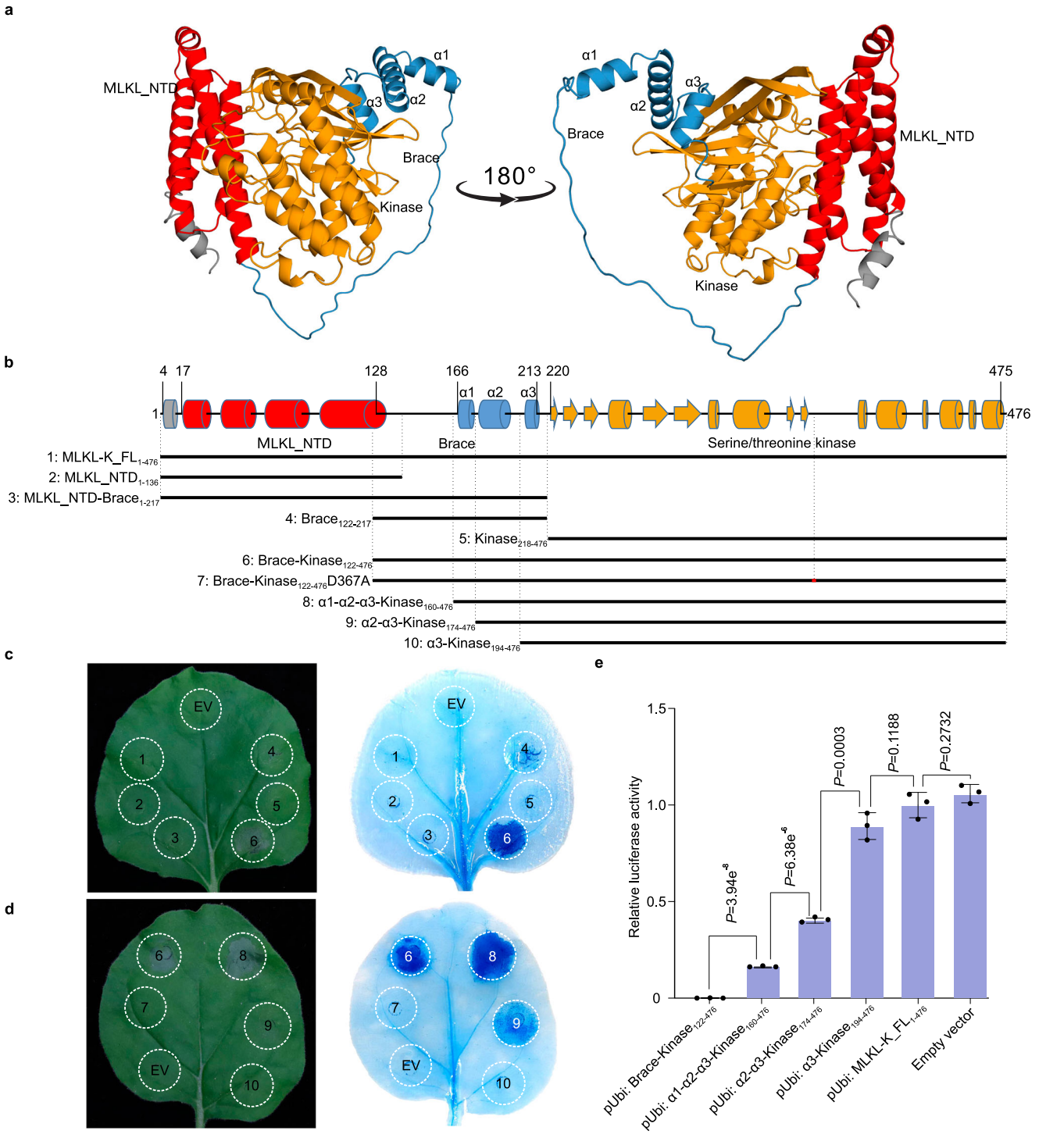

Fig. 3 | Protein structure prediction and functional analysis of MLKL-K. **a**, Three-dimensional model of MLKL-K predicted by AlphaFold v2.0. Red: MLKL_NTD domain, blue: brace region, orange: serine/threonine kinase domain, and gray: unidentified protein region. **b**, Secondary structure of MLKL-K illuminated by cylinders (α-helixes) and arrows (β-sheets). Colors represent protein domains as described above. Black bars represent constructs containing the corresponded MLKL-K expression cassettes. **c, d**, Cell death in *N. benthamiana* leaves at 48 h after infiltration with *Agrobacterium tumefaciens* carrying constructs of *35 S* promoter-driven *MLKL-K* fragments 1 to 10 illuminated above. Quantitative data corresponding to Fig. 3d are presented in Supplementary Fig. 14. EV: empty vector. Both experiments were performed on at least ten *N. benthamiana* leaves with similar results. **e**, Relative luciferase activity of wheat protoplasts measured at 16 h after co-transformation with indicated constructs and a construct carrying a luciferase reporter gene. Relative luciferase activity values are means ± SD from three biological replicates. Error bars represent standard deviations of three biological replicates. The relative fluorescence intensity of luciferase was used to assess cell viability. *P* values were calculated with a two-tailed Student's *t*-test. The experiment was independently repeated three times with similar results. Source data are provided as a Source Data file.

of human and mouse, which retains a self-inhibition state through intramolecular interaction between the pseudokinase and 4HB/MLKL_NTD domains[59]. The phosphorylation of the pseudokinase domain of MLKL by an upstream kinase RIPK3 triggers a molecular switch, leading to exposure of the 4HB/MLKL_NTD domain and brace-mediated oligomerization of the 4HB//MLKL_NTD domain. Subsequent plasma membrane translocation and permeabilization trigger cell death[59–61]. The expression of the 4HB plus the brace region of AtMLKLs or the 4HB alone of mouse MLKL was sufficient to induce cell death[57,59]. We found that the expression of either the 4HB or the 4HB plus the brace region of MLKL-K/Pm13 did not induce cell death, while the expression of Brace-kinase$_{122\text{-}476}$ of MLKL-K/Pm13 induced strong cell death, which relies on a functional kinase domain and the three helices in the brace region. As kinase catalytic activation usually depends on its dimerization-dependent autophosphorylation[62,63], the three helices in the brace region of MLKL-K might facilitate dimerization and activation of its kinase domain. Since the full-length MLKL-K did not induce any cell death, it is suggested that the MLKL_NTD domain might prevent dimerization of the kinase domain and maintain an inactively primed state. We hypothesize that MLKL-K/Pm13 might also stay in a self-inhibition state through intramolecular interaction between the 4HB/MLKL_NTD and kinase domains, or an auto-repressed state through intermolecular interactions. Unlike AtMLKLs and animal MLKLs, the putative functional kinase domain of MLKL-K/Pm13, rather than its 4HB/MLKL_NTD domain, is responsible for triggering cell death.

A disease resistance protein is a double-edged sword for host plants. It is able to prevent pathogen invasion but can also cause damage. Therefore, the activity of disease resistance protein needs to be stringently self-regulated. For instance, NLR-mediated resistance, relying on induced cell death upon pathogen infection, maintains a self-inhibition state through intramolecular interactions and can be switched into an activated state upon recognition of pathogen effector[64]. Yu et al. [36] proposed that KFPs may function through NLR-based and non-NLR-based decoy models. The NLR-based model suggests that KFP may serve as a decoy of an NLR guard. In this case, KFPs are sensors that perceive pathogen effectors and conduct the defense signal to executor NLR, and then trigger cell death. In the non-NLR-based model, KFPs stay in a self-inhibition state until the perception of pathogen effectors[36]. In this case, KFPs are both sensors that perceive pathogen effectors and executors induce cell death. Our results indicate that MLKL-K might function through the non-NLR-based decoy model, in which MLKL-K stays in a primed self-inhibition state prior to *Bgt* infection. Its N-terminal MLKL-NTD domain might serve as a decoy, which recognizes the *Bgt* effector and subsequently activates the kinase domain, initiates defense signal transduction, induces cell death, and ultimately prevents the colonization of the *Bgt* pathogen.

Methods

Plant materials and growth conditions

Wheat-*Ae. longissima* chromosome translocation line R1A carries the powdery mildew resistance gene *Pm13* on the terminal region of the chromosomal arm 3S^{l}S[12–15]. Line No. 3778 was derived from the cross and backcross between R1A and wheat cv. Bainong3217 with a pedigree of R1A/Bainong3217*5. Here, line No. 3778 was crossed with powdery mildew-susceptible cultivar XM44 to generate F_1 plants and a segregating F_2 population. Yangmai 18 (YM18), which carries *Pm21* on the wheat-*Dasypyrum villosum* translocated chromosome T6AL·6VS, has broad-spectrum resistance to powdery mildew[65] and was used as a resistant control. The powdery mildew-susceptible wheat accession Fielder was used as the recipient for genetic transformation. Twenty-one *Ae. longissima* accessions were ordered from the U.S. National Plant Germplasm System (NPGS) and Genebank Information System of the IPK Gatersleben (GBIS-IPK). *Nicotiana benthamiana* was used for transient expression assay. Susceptible wheat cultivar Yangmai 23 (YM23) was used for reproducing conidiospores of *Bgt*. Plants were grown on KLASMAN compost supplied with proper slow-release fertilizer in a greenhouse with ZK-TB18-DH01 LED lighting (~5000 Lux) under long-day conditions (16 h light/8 h dark) at 24 °C.

ND-FISH analysis

Root tips of line No. 3778 and Chinese Spring were treated with nitrous oxide for 2 h and fixed with 90% acetic acid for 10 min[66]. After washing with double distilled water, root tips were digested with 1% pectolyase and 2% cellulase solution (Yakult Pharmaceutical Industry Co., Ltd, Tokyo, Japan)[41]. The ND-FISH assay was performed on mitotic metaphase cells using oligo-nucleotide probes, Oligo-pSc119.2[67], and Oligo-pTa535[68], labeled with 6-carboxyflfluorescein (FAM) and 6-carboxytetramethylrhodamine (TAMRA), respectively, followed by staining with 4′, 6-diamidino-2-phenylindole to identify individual chromosomes[69]. At least three metaphase plates per seedling were analyzed, and FISH images were captured using a Leica DM2500 microscope equipped with a cooled charge-coupled device camera operated with LAS Live software (version 4.6) (Leica, Wetzlar, Germany).

Phenotypic assessments of powdery mildew resistance

Wheat plants, including the parents, F_1 (8 plants) and F_2 (238 plants), were inoculated with *Bgt* isolate BgtYZ01 by dusting fungal conidiospores onto leaves at the one-leaf stage. Powdery mildew reactions at the seedling stage were assessed at 7 days post inoculation (dpi). Infection types (ITs) were scored on a 0–4 scale, where, ITs 0, 0; 1 and 2 were regarded as resistant, and ITs 3 and 4 as susceptible[70]. The resistance spectrum of line No. 3778 carrying *Pm13* was examined in seedling tests with three replicates using a set of 108 *Bgt* isolates held in Institute of Plant Protection and Soil Science, Hubei Academy of Agricultural Sciences, Wuhan, China. Among them, 101 isolates were collected from different regions of China[17–19] and the other seven (07004, 94202, 96224, 97235, 98013, 98250 and JIW2) were from Europe[3]. YM18 carrying *Pm21* and Chancellor (CC) without any *Pm* gene were used as the resistant and susceptible controls, respectively. Specifically, leaves of No. 3778, YM18 and CC were cut into segments 3 cm in length and placed in Petri dishes containing 3.0 g/L agar and 50 mg/L 6-benzylaminopurine (6-BA). Line No. 3778 and Fielder were used as the resistant and susceptible controls, respectively. Three biological replicates of each line were adopted. Leaves embed in Petri dishes were inoculated with one *Bgt* isolate, maintained ex vivo at 18 °C on 16 h light/8 h dark cycle. At 10 dpi, responses to powdery mildew were then assessed using the 0–4 scale as described above. Eight representative isolates were used to reassess the responses of No. 3778, YM18 and CC seedlings (with at least 10 plants for each line) at the one-leaf stage. To detect the adult-plant resistance in the field, flag leaves of No. 3778 were inoculated with *Bgt* isolate BgtYZ01. YM18 and XM44 were used as the resistant and susceptible controls, respectively.

Molecular marker analysis

Ninety primer pairs were designed according to 57 single copy or low copy genes within the *Pm13* translocated chromosomal segment of *Ae. longissima* accession AEG-6782-2 (physical position: 0–24 Mb)[71]. Amplification of DNA was performed using the genomic DNA of line No. 3778 and XM44 as templates in a T100 thermal cycler (Bio-Rad, Hercules, CA, USA) with an initial denaturation at 94 °C for 3 min, 35 cycles of 10 s at 94 °C, 30 s at 55 °C, 1 min at 72 °C, and a final extension for 5 min at 72 °C. Reaction mixtures (25 µl) were composed of 1× PCR buffer, 0.2 mM of each dNTP, 2 µM of each primer, 50 ng genomic DNA, and 1 Unit of rTaq DNA polymerase (TaKaRa, Shiga, Japan, Catalog No. R001A). Products amplified were separated in 8% non-denaturing polyacrylamide gels and visualized after silver staining. Thirty-seven polymorphic markers (Supplementary Data 2) were detected with either size differences or present-absent differences. The diagnostic marker *XMLKL-K* was developed from the identified

transcript NODE_25350. Products were amplified with the above PCR conditions and visualized by 1.2% agarose gel electrophoresis.

Genetic analysis and physical mapping

Phenotypes of the F_2 population containing 238 plants from the cross between line No. 3778 and XM44 were assessed as described above. Four co-dominant markers, *X1650*, *X3140*, *X3990*, and *X5730*, spanning ~16 Mb of the chromosomal arm 3S^{l}S, were used to genotype the F_2 population. Genotypic and phenotypic results are shown in Supplementary Data 3. The Chi-squared (χ^2) test was performed to determine the goodness-of-fit of the observed segregation ratio to the theoretical Mendelian ratio.

About 800 dry seeds of line No. 3778 were irradiated with ^{60}Co-γ-ray with 200 Gy with a dosage rate of 1.0 Gy/min[19,39]. Irradiated seeds were sown in the field, and 424 M_2 families were harvested. About 50 seeds of each M_2 families were sown in greenhouse conditions as described above and inoculated with BgtYZ01 at the one-leaf stage. Ten independent susceptible mutants (m1 to m10) were obtained from different M_2 families. Then, about 20 M_3 one-leaf-stage seedlings from each M_2 family were inoculated with BgtYZ01 to confirm their phenotypes. The genomic DNA of each mutant was extracted and used as templates in amplification with the 37 polymorphic markers to physically map *Pm13*.

Transcriptome sequencing and analysis

About 500 seeds of line No.3778 were soaked in 0.05 M PBS solution for 4 h at 22 °C and then treated with 0.05 M PBS solution containing 0.6% ethyl methanesulfonate (EMS) for 10 h at 22 °C, followed by washing in running water for 4 h. The treated seeds were sown in the field and 326 M_2 families were harvested. Approximately 50 seedlings of each M_2 family were inoculated with BgtYZ01 as described above. Susceptible mutants were allowed to produce seeds in single pots. About 20 M_3 seeds of each independent mutant were re-assessed for their reactions to isolate BgtYZ01. Seedlings of line No. 3778 and six phenotype-confirmed mutants at the four-leaf stage were inoculated with BgtYZ01. As the expression of powdery mildew resistance genes usually peaked at 6 to 24 hpi[19,33,65,72,73], we collected the third and fourth leaves at 24 hpi for total RNAs extraction using the RNAiso Plus Kit (TaKaRa, Shiga, Japan, Catalog No. 9109). The quality and quantity of RNA purified were determined using a Nanodrop ND-1000 spectrophotometer (NanoDrop Technologies, Wilmington, DE, USA, Catalog No. E7530). Qualified RNA samples were used for library construction with the NEBNext Ultra RNA Library Prep Kit (NEB, Ipswich, MA, USA, Catalog No. E7530). RNA-Seq analysis was carried out on an Illumina platform with the PE150 strategy at Novogene Bioinformatics Technology Co., Ltd (Beijing, China).

The RNA-Seq analysis produced an average 72.2 million Illumina reads (2 × 150 bp) for the mutants. Data generated by RNA-Seq of the WT were assembled using SPAdes (v.3.15.3) with default parameters[74]. The outcome file 'transcripts.fasta' containing 201,798 transcripts was used as an input for the remaining steps of the MutIsoSeq pipeline[20]. Briefly, transposable elements were masked by Repeatmasker (v.4.0.7; http://www.repeatmasker.org) using the TREP database (v.2019)[75] as an external library. SeqKit (v2.2.056)[76] was used to sort the transcripts from the longest to the shortest. The sorted fasta file was used as a reference to map the Illumina reads from the susceptible mutants using BBMap (v.38.96)[77]. The resulting sam files were sorted, indexed, and converted to the mpileup format using samtools (v1.6)[78]. The pileup files were converted to xml files using Pileup2XML.jar and used as inputs to generate the final report using MutChromSeq.jar[22].

Gene isolation

The genomic sequence of *MLKL-K* was amplified from line No. 3778 using the primer pair P1/P2 designed according to transcript NODE_25350 and subsequently sequenced by Sanger sequencing. The upstream and downstream sequences of *MLKL-K* were isolated through PCR amplification using the primer pairs P3/P4 and P5/P6, respectively, designed based on the conserved sequences of the Sitopsis species of *Aegilops*. Total RNA was extracted from the third and the fourth leaves of line No. 3778 challenged by *Bgt* isolate BgtYZ01 (24 hpi) using the RNAiso Plus Kit (TaKaRa, Shiga, Japan, Catalog No. 9109). Total RNA (2 μg) was used for the synthesis of the first-strand cDNA using the PrimeScript™ II 1st Strand cDNA Synthesis Kit (TaKaRa, Shiga, Japan, Catalog No. 6210A). The transcript of *MLKL-K* was confirmed by RT-PCR and Sanger sequencing. The *MLKL-K* alleles from different *Ae. longissima* accessions were amplified from corresponding cDNAs by RT-PCR using the primer pair P7/P8, followed by Sanger sequencing. All amplifications were carried out using the high-fidelity PrimeSTAR GXL DNA polymerase (TaKaRa, Shiga, Japan, Catalog No. R050A).

Sequence and evolutionary analyses

The three-dimensional structure of MLKL-K was predicted by AlphaFold v2.0[79]. The amino acid sequence of the MLKL_NTD domain of MLKL-K was used to perform a BLAST search against the published Triticeae proteomes collected on the WheatOmics website (http://202.194.139.32/)[80] and the proteomes of other species in Phytozome website (https://phytozome-next.jgi.doe.gov) (Supplementary Data 9). The domains of the matched proteins were predicted in the conserved domain database of NCBI. In total, 298 putative kinase and pseudokinase domains of plant tandem kinase proteins, Triticeae kinase fusion proteins[20,36], Triticeae MLKL-K-like proteins, Sitopsis MLKL-K proteins, *Arabidopsis* MLKLs[57], and human MLKL[59] were used for phylogenetic analysis using the neighbor-joining method with a bootstrap 10,000 by MEGA 7 (https://www.megasoftware.net/). Multiple sequence alignment was applied using ClustlW of MEGA 7. The exported Newick tree file was illuminated using iTOL (https://itol.embl.de/).

Single-cell transient assay in wheat leaves

The full-length *MLKL-K* CDS was amplified from cDNA of line No. 3778 using high-fidelity PrimeSTAR GXL DNA polymerase (TaKaRa, Shiga, Japan, Catalog No. R050A), inserted into the entry vector pDONR207 to produce pDONR207-*MLKL-K*-CDS, and confirmed by Sanger sequencing with primers provided in Supplementary Data 6. Then, the *MLKL-K* CDS in pDONR207-*MLKL-K*-CDS was used to generate the recombinant plasmid pUbi-*MLKL-K*-CDS using Gateway™ LR Clonase™ II Enzyme mix (Thermo Fisher, Carlsbad, CA, USA, Catalog No. 11791-100). The mixture of the recombinant plasmid pUbi-*MLKL-K*-CDS and reporter vector pUbi:GUS was co-transferred into leaves of the susceptible wheat cv. XM44 uses a helium-driven particle delivery system (BioRad, Hercules, CA, USA). Briefly, gold particles (BIO-RAD, Hercules, CA, USA, Catalog No. 1652263) coated with the plasmid mixture were introduced into epidermal cells of detached leaves using the particle inflow gun (PIG) system[81,82]. The constructs carrying *Pm21* (positive) and the empty vector (negative) were also co-transferred with pUbi:GUS into XM44 leaves. In each test group, particle bombardment was carried out on 17–18 leaves. Leaves were then inoculated with avirlent *Bgt* isolate E09 at 4 h after bombardment and stained with the GUS solution at 48 hpi to observe the haustorium structure of *Bgt* under a microscope. The haustorium index, i.e., the percentage of GUS-staining cells with haustoria among all GUS-stained cells invaded by the *Bgt* pathogen, was determined to assess whether *MLKL-K* could provide the powdery mildew resistance transiently. Statistical analysis was done using a two-tailed *t*-test.

Wheat transformation

The *MLKL-K* CDS (1431 bp), along with the upstream sequence (2637 bp) and downstream sequence (1932 bp), was synthesized at GENEWIZ (Suzhou, China) and ligated into the binary vector pLGY03. The resultant construct was used for *Agrobacterium tumefaciens*-mediated transformation of susceptible wheat cv. Fielder[83]. Seven T_0

plants generated were tested for the presence of the transgenic component by PCR using the marker *XMLKL-K*. Line No. 3778 and non-transgenic Fielder were used as positive and negative controls, respectively. To evaluate the expression level of *MLKL-K* in transgenic wheat lines, total RNA was extracted from the first leaves of three transgene-positive T_1 plants derived from each of the seven T_0 plants. The RNA samples were used to synthesize the first strand of cDNA as described above. Quantitative RT-PCR (qPCR) was performed using primer pair QMLKL-K-F/R and above cDNA as a template. Gene *actin* was used as the endogenous control. Three technical replicates were performed for each cDNA sample. The $2^{-\Delta\Delta Ct}$ method was used to normalize and calibrate transcript values relative to the endogenous *actin* control[84]. Line No. 3778 was used as a control to indicate the expression level of native *MLKL-K*.

Phenotypic assessment of transgenic wheat lines

Firstly, seven T_0 transgenic wheat lines at the booting stage were inoculated with isolate BgtYZ01 in a greenhouse, and phenotypes of the flag leaves were observed at 14 dpi. Secondly, ten T_1 plants derived from each T_0 line were phenotyped by inoculating with BgtYZ01 at the one-leaf stage and genotyped with the diagnostic marker *XMLKL-K*. Thirdly, T_1 lines 1 and 2 containing *MLKL-K* were obtained after PCR with marker *XMLKL-K*. Leaf segments of these two lines were used to test reactions to 20 *Bgt* isolates collected from different regions using the ex vivo method described above. Line No. 3778 and Fielder were used as the resistant and susceptible controls, respectively. Three biological replicates of each wheat line were adopted.

Histochemical detection of H_2O_2 and cell death in wheat leaves

Line No. 3778 and XM44 were inoculated with avirulent *Bgt* isolate E09 at the one-leaf stage. At 48 hpi, leaves were treated in 3,3′-diaminobenzidine (DAB) staining solution (1 mg/ml DAB-HCl, 10 mM Na_2HPO_4, and 0.05% v/v Tween-20) for 8 h and destained in 90% ethanol. At 60 hpi, leaves were collected and immersed in a trypan blue staining solution (2.5 mg/ml trypan blue, 25% lactic acid, and 23% saturated phenol) for 30 min in boiling water. Chloral hydrate solution (2.5 g/ml) was used to destain for 3 d. The above leaf samples were stained with 0.6% Comassie brilliant blue R-250 solution for 10 s to observe *Bgt* spore and hypha using a Leica DM2500 microscope (Leica, Wetzlar, Germany). In such experiments, the presence of *Bgt* spores did not consistently associate with H_2O_2 accumulation and induced cell death in epidermal cells of line No. 3778 and XM44. Only a small proportion of spores triggered such immune responses in the *Pm13* donor line No. 3778, while almost no cell death or H_2O_2 accumulation was observed in the susceptible control XM44. Representative images were taken using a Leica DM2500 microscope (Supplementary Fig. 10).

Transgene-positive and negative siblings of T_1-line4 to T_1-line7, along with the WT Fielder plants, were grown until the heading stage in a greenhouse with long-day conditions (16 h light/8 h dark, 21 °C). The matured second leaves below flag leaves were used for trypan blue staining following the procedure described above. Stained leaves were scanned on an Epson Perfection V850 Pro scanner. Photos of whole plants were taken using a Canon EOS 6D (W) camera.

Cell death assay on *N. benthamiana* leaves

The full-length *MLKL-K* CDS and its partial fragments were amplified from No. 3778 cDNA using high fidelity PrimeSTAR GXL DNA polymerase (TaKaRa, Shiga, Japan, Catalog No. R050A), digested with *Sma*I and *Kpn*I, and inserted into the vector pS1300-GFP-Nos (C-terminal fused GFP) and pS1300[85,86] to generate *35 S* promoter-driven MLKL-K and truncated fragments with or without C-terminal fused GFP. MLKL-K with N-terminal fused GFP was generated by assembling PCR fragments of *GFP* (without termination codon) and *MLKL-K* into pS1300 using the ClonExpress Ultra One Step Cloning Kit (Vazyme, Nanjing, China, Catalog No. C115-01). To create a dead kinase gene *Brace-Kinase*$_{122\text{-}476}$*D367A*, the nucleotide A at position 1100 in the *MLKL-K* CDS was altered to C using overlap extension PCR[87], which leads to an amino acid substitution of aspartate (D) with alanine (A) at position 367[88,89]. *Brace-Kinase*$_{122\text{-}476}$*G401D*, *Brace-Kinase*$_{122\text{-}476}$*G308E*, *Brace-Kinase*$_{122\text{-}476}$*G231R*, *Brace-Kinase*$_{122\text{-}476}$*P461L* and *Brace-Kinase*$_{122\text{-}476}$*C334Y* were amplified from the cDNA samples of *Bgt*-susceptible mutants m11, m12, m13, m15 and m16, respectively. The *Brace-Kinase*$_{122\text{-}476}$ fragments with point mutations were also cloned into pS1300 independently. All constructs were confirmed by Sanger sequencing. Primers used for constructs are listed in Supplementary Data 6. *Agrobacterium* strain GV3101 carrying the above construct was grown at 28 °C in Luria Bertani (LB) broth, harvested by centrifugation, and suspended in infiltration buffer [2% sucrose, 0.5% Murashige & Skoog basal salts, 10 mM 2-(N-morpholine)-ethanesulfonic acid, pH 5.6, and 200 µM acetosyringone]. The suspension was diluted to OD_{600} of 0.8 using the above infiltration buffer and incubated for 1–3 h at room temperature. Ten *N. benthamiana* leaves were infiltrated with each suspension and photographed at 48 h after infiltration. The infiltrated leaves were stained in a trypan blue solution (10 ml lactic acid, 10 ml glycerol, 10 g phenol, 10 mg trypan blue, and 50 ml ethanol, dissolved in 30 ml distilled water) in boiling water for 5 min. The stained leaves were soaked in chloral hydrate solution (2.5 g/ml) until the background disappeared. In the above cell death assay, *Agrobacterium* strain GV3101 harboring the empty vector pS1300 was used as a negative control.

Western blotting analysis

Using the same method as above, the full-length *MLKL-K* and its partial fragments were inserted into the vector pS1300-GFP-Nos, which allows for creating fusions with GFP on the C-terminus of target fragments. *Agrobacterium* strain GV3101 carrying constructs expressing the GFP-fused protein was infiltrated into *N. benthamiana* leaves. At 20 h post infiltration, total proteins were extracted from 0.1 g of fresh leaves using Plant Protein Extraction Kit (CWBIO, Taizhou, China, Catalog No. CW0885M). The lysates were centrifuged at 12,000 × *g* for 20 min (4 °C). Supernatants were collected and incubated with 5× SDS loading buffer at 95 °C for 5 min. Heated protein samples were separated by 12% (w/v) sodium dodecyl sulfate-polyacrylamide gel electrophoresis (SDS-PAGE) gel and transferred to a PVDF membrane. Immunoblots were detected with an anti-GFP antibody. The primary antibody used for the identification of GFP and GFP fusion proteins was Anti-GFP (Proteintech, Wuhan, China, Catalog No. 66002-1-lg) at a dilution of 1:5000. Following that, the secondary antibody used to detect the primary antibody was HPR-conjugated Affinipure Goat Anti-Mouse IgG (Proteintech, Wuhan, China, Catalog No. SA00001-1) at a dilution of 1:5000. Equal loading was controlled by probing with an anti-Actin antibody.

Quantitative analysis of cell death activity in wheat protoplasts

Protoplasts were isolated from the second leaves of wheat cultivar Fielder. Briefly, the second leaves of 2 weeks Fielder seedlings were harvested, and after removing epidermis, the leaves were placed into protoplast isolation buffer with 15 mg/ml Cellulase R-10 (YAKULT Honsha, Tokyo, Japan, Catalog No. L0012) and 5 mg/ml Macerozyme R-10 (YAKULT Honsha, Tokyo, Japan, Catalog No. L0021), incubated for 3 hours at room temperature in dark with shaking at 60 rpm. Wheat protoplasts were harvested by filtration and centrifugation[90]. The full-length *MLKL-K* CDS and its partial fragments were first ligated into entry vector pDONR207 and then recombined into a maize *ubiquitin* promoter-driven vector, pUbi-GW, using Gateway™ LR Clonase™ II Enzyme mix (Thermo Fisher, Carlsbad, CA, USA, Catalog No. 11791-100). All final constructs were confirmed by Sanger sequencing using primers provided in Supplementary Data 6. The mixture of each construct (10 µg) and the luciferase (LUC) reporter vector (10 µg) were transformed into the protoplasts prepared using the method reported by Saur et al.[90]. After overnight incubation at 22 °C in darkness, the transformed protoplasts were collected by centrifugation, suspended

in 0.2 mL 2× Cell Culture Lysis Buffer (Promega, Madison, WI, USA, Catalog No. E153A), and mixed with an equal volume of Luciferase Assay Substrate (Promega, Madison, WI, USA, Catalog No. E151A). The LUC activity of the samples was immediately detected using Glo-Max®96 Microplate Luminometer (Promega, Madison, WI, USA). The empty vector pUbi-GW mixed with LUC reporter vector was used as a control. The above experiment was carried out three times. Since only live transformed cells could express luciferase, which emits fluorescence once the substrate is provided, the relative fluorescence intensity of LUC was used to assess cell viability.

Subcellular localization of MLKL-K

Protoplasts were isolated from the second leaves of wheat cultivar Fielder as described above. The *Arabidopsis* histone gene *AtH2B* was amplified from *Arabidopsis* Col-0 cDNA using high fidelity PrimeSTAR GXL DNA polymerase (TaKaRa, Shiga, Japan, Catalog No. R050A), digested with *Kpn*I and *BamH*I, and inserted into the vector pCAMBIA2300-RFP (C-terminal fused RFP), generating construct pCAMBIA2300-AtH2B-RFP. The constructs pS1300-MLKL-K-GFP-Nos (10 μg) and pS1300-GFP-Nos (10 μg) were separately mixed with 10 μg of pCAMBIA2300-AtH2B-RFP. The mixtures were transformed into the protoplasts prepared using the method reported by Saur et al.[90]. Fluorescence images were taken at 12 h after transfection using a Nikon confocal microscope (LSM980, Zeiss, city, Germany). GFP fluorescence was excited with a 488 nm laser recorded with 490–552 nm wavelength of light. RFP fluorescence was excited with a 558 nm laser and detected with 560–620 nm wavelength of light. For mCherry, fluorescence was excited with a 587 nm laser and detected with 572–658 nm wavelength of light. For the subcellular localization of MLKL-K in *N. benthamiana* epidermic cells, *Agrobacteria* carrying constructs pS1300-MLKL-K-GFP-Nos and pS1300-GFP-Nos were separately co-infiltrated with *Agrobacteria* carrying construct pS1300-mCherry-Nos into *N. benthamiana* leaves as described above. At 12 h post infiltration, fluorescence images were acquired following the confocal microscope setting described above.

Reporting summary

Further information on research design is available in the Nature Portfolio Reporting Summary linked to this article.

Data availability

Data supporting the findings of this work are available within the paper and its Supplementary Information files. Datasets generated and analyzed during the current study are available from the corresponding author upon request. RNA-Seq data from the *Bgt*-infected leaves of the WT line No. 3778 and its mutants can be found in the European Nucleotide Archive (ENA) under the accession number PRJEB63085. The transcriptome assembly of the WT line No. 3778 was deposited in the ENA under the accession number HCEC01000000. The sequence of *Pm13* from wheat line No. 3778 and its alleles from *Ae. longissima* accessions were deposited in the Genbank of NCBI under the accession numbers OR052510-[OR052527]. The transcriptome assembly of the WT line No. 3778, sequences of the transcript NODE_25350 and the CDS, and the genomic sequence of *Pm13* are also available on the DRYAD database [https://doi.org/10.5061/dryad.qjq2bvqmz]. Source data are provided with this paper.

References

1. Singh, R. P. et al. Disease impact on wheat yield potential and prospects of genetic control. *Annu. Rev. Phytopathol.* **54**, 303–322 (2016).
2. Morgounov, A. et al. Global incidence of wheat rusts and powdery mildew during 1969–2010 and durability of resistance of winter wheat variety Bezostaya 1. *Eur. J. Plant Pathol.* **132**, 323–340 (2012).
3. Sotiropoulos, A. G. et al. Global genomic analyses of wheat powdery mildew reveal association of pathogen spread with historical human migration and trade. *Nat. Commun.* **13**, 4315 (2022).
4. Zou, Y. F. et al. Regionalization of wheat powdery mildew oversummering in China based on digital elevation. *J. Integr. Agr.* **17**, 901–910 (2018).
5. Kunz, L. et al. The broad use of the *Pm8* resistance gene in wheat resulted in hypermutation of the *AvrPm8* gene in the powdery mildew pathogen. *BMC Biol.* **21**, 29 (2023).
6. Müller, M. C. et al. A chromosome–scale genome assembly reveals a highly dynamic effector repertoire of wheat powdery mildew. *New Phytol.* **221**, 2176–2189 (2019).
7. He, H. G. et al. Characterization of a new gene for resistance to wheat powdery mildew on chromosome 1RL of wild rye *Secale sylvestre*. *Theor. Appl. Genet.* **134**, 887–896 (2021).
8. Kuluev, A. R., Kuluev, B. R. & Chemeris, A. V. The problem of the origin of subgenomes B, A, and D of bread wheat (*Triticum aestivum* L.): old facts and new evidences. *Biol. Bull. Rev.* **13**, 148–161 (2023).
9. Li, L. F. et al. Genome sequences of five Sitopsis species of *Aegilops* and the origin of polyploid wheat B subgenome. *Mol. Plant* **15**, 488–503 (2022).
10. Huang, S. Y., Steffenson, B. J., Sela, H. & Stinebaugh, K. Resistance of *Aegilops longissima* to the rusts of wheat. *Plant Dis.* **102**, 1124–1135 (2018).
11. Sheng, H. Y. & Murray, T. D. Identifying new sources of resistance to eyespot of wheat in *Aegilops longissima*. *Plant Dis.* **97**, 346–353 (2013).
12. Ceoloni, C., Signore, G. D., Ercoli, L. & Donini, P. Locating the alien chromatin segment in common wheat–*Aegilops longissima* mildew resistant transfers. *Hereditas* **116**, 239–245 (1992).
13. Cenci, A., D'Ovidio, R., Tanzarella, O. A., Ceoloni, C. & Porceddu, E. Identification of molecular markers linked to *Pm13*, an *Aegilops longissima* gene conferring resistance to powdery mildew in wheat. *Theor. Appl. Genet.* **98**, 448–454 (1999).
14. Cenci, A. et al. Genetic analysis of the *Aegilops longissima* 3S chromosome carrying the *Pm13* resistance gene. *Euphytica* **130**, 177–183 (2003).
15. Donini, P., Koebner, R. M. & Ceoloni, C. Cytogenetic and molecular mapping of the wheat–*Aegilops longissima* chromatin breakpoints in powdery mildew-resistant introgression lines. *Theor. Appl. Genet.* **91**, 738–743 (1995).
16. Li, H. H. et al. Development of novel wheat-*Aegilops longissima* $3S^{l}$ translocations conferring powdery mildew resistance and specific molecular markers for chromosome $3S^{l}$. *Plant Dis.* **105**, 2938–2945 (2021).
17. Bourras, S. et al. The *AvrPm3–Pm3* effector–NLR interactions control both race–specific resistance and host–specificity of cereal mildews on wheat. *Nat. Commun.* **10**, 2292 (2019).
18. Zeng, F. S. et al. Virulence and diversity of *Blumeria graminis* f. sp. *tritici* populations in China. *J. Integr. Agr.* **13**, 2424–2437 (2014).
19. Zhu, S. Y. et al. Orthologous genes *Pm12* and *Pm21* from two wild relatives of wheat show evolutionary conservation but divergent powdery mildew resistance. *Plant Commun.* **4**, 100472 (2023).
20. Wang, Y. J. et al. An unusual tandem kinase fusion protein confers leaf rust resistance in wheat. *Nat. Genet.* **55**, 914–920 (2023).
21. Slade, A. J., Fuerstenberg, S., Loeffler, D., Steine, M. N. & Facciotii, D. A reverse genetic, nontransgenic approach to wheat crop improvement by TILLING. *Nat. Biotechnol.* **23**, 75–81 (2005).
22. Sánchez-Martín, J. et al. Rapid gene isolation in barley and wheat by mutant chromosome sequencing. *Genome Biol.* **17**, 221 (2016).
23. Klymiuk, V., Coaker, G., Fahima, T. & Pozniak, C. Tandem protein kinases emerge as new regulators of plant immunity. *Mol. Plant-Microbe Interact.* **34**, 1094–1102 (2021).

24. Arora, S. et al. A wheat kinase and immune receptor form host–specificity barriers against the blast fungus. *Nat. Plants* **9**, 385–392 (2022).
25. Brueggeman, R. et al. The stem rust resistance gene *Rpg5* encodes a protein with nucleotide–binding–site, leucine–rich, and protein kinase domains. *Proc. Nat. Acad. Sci. USA* **105**, 14970–14975 (2008).
26. Brueggeman, R. et al. The barley stem rust-resistance gene *Rpg1* is a novel disease-resistance gene with homology to receptor kinases. *Proc. Nat. Acad. Sci. USA* **99**, 9328–9333 (2002).
27. Chen, S. S. et al. Wheat gene *Sr60* encodes a protein with two putative kinase domains that confers resistance to stem rust. *New Phytol.* **225**, 948–959 (2020).
28. Faris, J. D. et al. A unique wheat disease resistance–like gene governs effector–triggered susceptibility to necrotrophic pathogens. *Proc. Nat. Acad. Sci. USA* **107**, 13544–13549 (2010).
29. Fu, D. L. et al. A Kinase-START gene confers temperature-dependent resistance to wheat stripe rust. *Science* **323**, 1357–1360 (2009).
30. Gaurav, K. et al. Population genomic analysis of *Aegilops tauschii* identifies targets for bread wheat improvement. *Nat. Biotechnol.* **40**, 422–431 (2021).
31. Hanks, S. K., Quinn, A. M. & Hunter, T. The protein kinase family: conserved features and deduced phylogeny of the catalytic domains. *Science* **241**, 42–52 (1988).
32. Klymiuk, V. et al. Cloning of the wheat *Yr15* resistance gene sheds light on the plant tandem kinase-pseudokinase family. *Nat. Commun.* **9**, 3735 (2018).
33. Lu, P. et al. A rare gain of function mutation in a wheat tandem kinase confers resistance to powdery mildew. *Nat. Commun.* **11**, 680 (2020).
34. Sánchez-Martín, J. et al. Wheat *Pm4* resistance to powdery mildew is controlled by alternative splice variants encoding chimeric proteins. *Nat. Plants* **7**, 327–341 (2021).
35. Yu, G. T. et al. *Aegilops sharonensis* genome-assisted identification of stem rust resistance gene *Sr62*. *Nat. Commun.* **13**, 1607 (2022).
36. Yu, G. T. et al. The wheat stem rust resistance gene *Sr43* encodes an unusual protein kinase. *Nat. Genet.* **55**, 921–926 (2023).
37. Zhang, Z. C. et al. A protein kinase–major sperm protein gene hijacked by a necrotrophic fungal pathogen triggers disease susceptibility in wheat. *Plant J.* **106**, 720–732 (2021).
38. Chen, P. D. et al. Radiation-induced translocations with reduced *Haynaldia villosa* chromatin at the *Pm21* locus for powdery mildew resistance in wheat. *Mol. Breed.* **31**, 477–484 (2013).
39. Zhang, J. et al. Identification of novel chromosomal aberrations Induced by $^{(60)}$Co–gamma–irradiation in wheat–*Dasypyrum villosum* lines. *Int. J. Mol. Sci.* **16**, 29787–29796 (2015).
40. Kolodziej, M. C. et al. A membrane-bound ankyrin repeat protein confers race-specific leaf rust disease resistance in wheat. *Nat. Commun.* **12**, 956 (2021).
41. Dracatos, P. M. et al. The coiled-coil NLR *Rph1*, confers leaf rust resistance in barley cultivar Sudan. *Plant Physiol.* **179**, 1362–1372 (2019).
42. Hewitt, T. et al. A highly differentiated region of wheat chromosome 7AL encodes a *Pm1a* immune receptor that recognizes its corresponding *AvrPm1a* effector from *Blumeria graminis*. *New Phytol.* **229**, 2812–2826 (2021).
43. Hewitt, T. et al. Wheat leaf rust resistance gene *Lr13* is a specific *Ne2* allele for hybrid necrosis. *Mol. Plant* **14**, 1025–1028 (2021).
44. Marchal, C. et al. BED-domain containing immune receptors confer diverse resistance spectra to yellow rust. *Nat. Plants* **4**, 662–668 (2018).
45. Steuernage, B. et al. Rapid cloning of disease-resistance genes in plants using mutagenesis and sequence capture. *Nat. Biotechnol.* **34**, 652–655 (2016).
46. Upadhyaya, N. M. et al. Genomics accelerated isolation of a new stem rust avirulence gene–wheat resistance gene pair. *Nat. Plants* **7**, 1220–1228 (2021).
47. Yan, X. C. et al. High–temperature wheat leaf rust resistance gene *Lr13* exhibits pleiotropic effects on hybrid necrosis. *Mol. Plant* **14**, 1029–1032 (2021).
48. Zhang, J. P. et al. A recombined *Sr26* and *Sr61* disease resistance gene stack in wheat encodes unrelated NLR genes. *Nat. Commun.* **12**, 3378 (2021).
49. Ni, F. et al. Sequencing trait-associated mutations to clone wheat rust resistance gene *YrNAM*. *Nat. Commun.* **14**, 4353 (2023).
50. Li, H. N. et al. Cloning of the wheat leaf rust resistance gene *Lr47* introgressed from *Aegilops speltoides*. *Nat. Commun.* **14**, 6072 (2023).
51. Lu, C. T. et al. Wheat *Pm55* alleles exhibit distinct interactions with an inhibitor to cause different powdery mildew resistance. *Nat. Commun.* **15**, 503 (2024).
52. Li, M. M. et al. A membrane associated tandem kinase from wild emmer wheat confers broad-spectrum resistance to powdery mildew. *Nat. Commun.* **15**, 3124 (2024).
53. Li, H. H. et al. Wheat powdery mildew resistance gene *Pm13* encodes a mixed lineage kinase domain-like protein. *Nat. Commun.* **15**, 2449 (2024).
54. Wang, G. X. et al. The decoy substrate of a pathogen effector and a pseudokinase specify pathogen-induced modified-self recognition and immunity in plants. *Cell Host Microbe* **18**, 285–295 (2015).
55. Cesari, S., Bernoux, M., Moncuquet, P., Kroj, T. & Dodds, P. N. A novel conserved mechanism for plant NLR protein pairs: the "integrated decoy" hypothesis. *Front. Plant Sci.* **5**, 606 (2014).
56. van der Hoorn, R. A. & Kamoun, S. From Guard to Decoy: a new model for perception of plant pathogen effectors. *Plant Cell* **20**, 2009–2017 (2008).
57. Mahdi, L. K. et al. Discovery of a family of mixed lineage kinase domain-like proteins in plants and their role in innate immune signaling. *Cell Host Microbe* **28**, 813–824 (2020).
58. Shen, Q. C. et al. Cytoplasmic calcium influx mediated by plant MLKLs confers TNL-triggered immunity. *Cell Host Microbe* **32**, 453–465 (2024).
59. Hildebrand, J. M. et al. Activation of the pseudokinase MLKL unleashes the four-helix bundle domain to induce membrane localization and necroptotic cell death. *Proc. Nat. Acad. Sci. USA* **111**, 15072–15077 (2014).
60. Quarato, G. et al. Sequential engagement of distinct MLKL phosphatidylinositol–binding sites executes necroptosis. *Mol. Cell* **61**, 589–601 (2016).
61. Tanzer, M. C. et al. Evolutionary divergence of the necroptosis effector MLKL. *Cell Death Differ.* **23**, 1185–1197 (2016).
62. Dey, M. et al. Mechanistic link between PKR dimerization, autophosphorylation, and eIF2α substrate recognition. *Cell* **122**, 901–913 (2005).
63. Rajakulendran, T., Sahmi, M., Lefrancois, M., Sicheri, F. & Therrien, M. A dimerization–dependent mechanism drives RAF catalytic activation. *Nature* **461**, 542–545 (2009).
64. Wang, J. Z. et al. Ligand–triggered allosteric ADP release primes a plant NLR complex. *Science* **364**, eaav5868 (2019).
65. He, H. G. et al. *Pm21*, encoding a typical CC–NBS–LRR protein, confers broad-spectrum resistance to wheat powdery mildew disease. *Mol. Plant* **11**, 879–882 (2018).
66. Zhang, J. et al. Molecular cytogenetic identification of the wheat–-*Dasypyrum villosum* T3DL.3V#3S translocation line with resistance against stripe rust. *Plants* **11**, 1329 (2022).
67. Cuadrado, A., Vitellozzi, F., Jouve, N. & Ceoloni, C. Fluorescence in situ hybridization with multiple repeated DNA probes applied to the analysis of wheat–rye chromosome pairing. *Theor. Appl. Genet.* **94**, 347–355 (1997).

68. Komuro, S., Endo, R., Shikata, K. & Kato, A. Genomic and chromosomal distribution patterns of various repeated DNA sequences in wheat revealed by a fluorescence in situ hybridization procedure. *Genome* **56**, 131–137 (2013).
69. Fu, S. L. et al. Oligonucleotide probes for ND–FISH analysis to identify rye and wheat chromosomes. *Sci. Rep.* **5**, 10552 (2015).
70. An, D. G. et al. Molecular cytogenetic characterization of a new wheat-rye 4R chromosome translocation line resistant to powdery mildew. *Chromosome Res.* **21**, 419–432 (2013).
71. Avni, R. et al. Genome sequences of three *Aegilops* species of the section Sitopsis reveal phylogenetic relationships and provide resources for wheat improvement. *Plant J.* **110**, 179–192 (2022).
72. Li, M. M. et al. A CNL protein in wild emmer wheat confers powdery mildew resistance. *New Phytol.* **228**, 1027–1037 (2020).
73. Xie, J. Z. et al. A rare single nucleotide variant in *Pm5e* confers powdery mildew resistance in common wheat. *New Phytol.* **228**, 1011–1026 (2020).
74. Bankevich, A. et al. SPAdes: a new genome assembly algorithm and its applications to single-cell sequencing. *J. Comput. Biol.* **19**, 455–477 (2012).
75. Wicker, T., Matthews, D. E. & Keller, B. TREP: a database for Triticeae repetitive elements. *Trends Plant Sci.* **7**, 561–562 (2002).
76. Shen, W., Le, S., Li, Y. & Hu, F. Q. SeqKit: a cross–platform and ultrafast toolkit for FASTA/Q file manipulation. *PLoS One* **11**, e0163962 (2016).
77. Bushnell, B. BBMap: a fast, accurate, splice–aware aligner. In *Proc. 9th Annual Genomics of Energy & Environment Meeting* (LBNL Department of Energy Joint Genome Institute) (2014).
78. Li, H. et al. The sequence alignment/map format and SAMtools. *Bioinformatics* **25**, 2078–2079 (2009).
79. Jumper, J. et al. Highly accurate protein structure prediction with AlphaFold. *Nature* **596**, 583–589 (2021).
80. Ma, S. W. et al. WheatOmics: a platform combining multiple omics data to accelerate functional genomics studies in wheat. *Mol. Plant* **14**, 1965–1968 (2021).
81. Shen, Q. H. et al. Nuclear activity of MLA immune receptors links isolate–specific and basal disease-resistance responses. *Science* **315**, 1098–1103 (2007).
82. Shirasu, K., Nielsen, K., Piffanelli, P., Oliver, R. & Schulze-Lefert, P. Cell-autonomous complementation of *mlo* resistance using a biolistic transient expression system. *Plant J.* **17**, 293–299 (1999).
83. Zhang, S. J. et al. Targeted mutagenesis using the *Agrobacterium tumefaciens*–mediated CRISPR–Cas9 system in common wheat. *BMC Plant Biol.* **18**, 302 (2018).
84. Livak, K. J. & Schmittgen, T. D. Analysis of relative gene expression data using real-time quantitative PCR and the $2^{-\Delta\Delta Ct}$ method. *Methods* **25**, 402–408 (2001).
85. Dong, H. et al. Modulation of guard cell turgor and drought tolerance by a peroxisomal acetate–malate shunt. *Mol. Plant* **11**, 1278–1291 (2018).
86. Gao, A. L. et al. Pm21 CC domain activity modulated by intramolecular interactions is implicated in cell death and disease resistance. *Mol. Plant Pathol.* **21**, 975–984 (2020).
87. Russell, H., Barbara, K. & Randall, S. A general method of in vitro preparation and specific mutagenesis of DNA fragments: study of protein and DNA interactions. *Nucleic Acids Res.* **16**, 7351–7367 (1988).
88. Jiang, Y. H. et al. MAP4K4 associates with BIK1 to regulate plant innate immunity. *EMBO Rep.* **20**, e47965 (2019).
89. Wang, Y. J. et al. Orthologous receptor kinases quantitatively affect the host status of barley to leaf rust fungi. *Nat. Plants* **5**, 1129–1135 (2019).
90. Saur, I. M. L., Bauer, S., Lu, X. & Schulze-Lefert, P. A cell death assay in barley and wheat protoplasts for identification and validation of matching pathogen AVR effector and plant NLR immune receptors. *Plant Methods* **15**, 118 (2019).

Acknowledgements

This study was supported by grants from National Key R&D Program of China (2022YFF1001500/2022YFF1001503 to Q.S.), National Natural Science Foundation of China (32171990 to H.H., 32172001 to H.L. and 32372507 to S.G.), Natural Science Foundation of Jiangsu Province (BK20231321 to H.H.) and State Key Laboratory of Plant Cell and Chromosome Engineering (PCCE-KF-2021-05 to H.H. and PCCE-KF-2022-07 to S.Z.), King Abdullah University of Science and Technology (to S.G.K.) and Center for Excellence in Molecular Plant Sciences, Chinese Academy of Sciences (start-up funding to Y.W.). The authors thank Dr. Genying Li of Crop Research Institution, Shandong Academy of Agricultural Sciences, Jinan, China for providing the binary vector pLGY03.

Author contributions

H.H., S.G.K., and Y.W. conceived and designed the research. H.H., Z.C., R.F., J.Z., S.Z., J.W., Q.Z., A.G., S.G., L.Z., Y.L. and Y.Z. performed experiments. H.H., Y.W., Z.C. and Q.S analyzed the data. H.H. and Y.W. wrote the manuscript with input from H.L. and S.G.K. H.H. and Z.C. contributed equally to this work.

Competing interests

The authors declare no competing interests.

Additional information

Supplementary information The online version contains supplementary material available at https://doi.org/10.1038/s41467-024-50909-6.

Correspondence and requests for materials should be addressed to Huagang He or Yajun Wang.

Peer review information *Nature Communications* thanks Matthew Moscou and the other, anonymous, reviewer(s) for their contribution to the peer review of this work. A peer review file is available.